GEOPHYSICAL RESEARCH LETTERS, VOL. ???, XXXX, DOI:10.1029/,

The signature of the Atlantic meridional overturning circulation in sea level along the east coast of North America

Rory J. Bingham

Proudman Oceanographic Laboratory, Liverpool, U.K.

Chris W. Hughes

Proudman Oceanographic Laboratory, Liverpool, U.K.

Rory J. Bingham, Chris W. Hughes, Proudman Oceanographic Laboratory, 6 Brownlow St., Liverpool L3 5DA, U.K. (rjbi@pol.ac.uk, cwh@pol.ac.uk)

In this letter we examine the relationship between the North Atlantic Meridional Overturning Circulation (MOC) and sea level (SL) along the east coast of North America. In the eddy permitting ocean model OCCAM we find a distinctive, topography-following pattern of SL variability in the western North Atlantic that is closely linked with the changing strength of the MOC, with a 2cm drop in SL along the US east coast corresponding to a 1Sv increase in the MOC. We find a similar pattern of SL variability in the altimetry record and show that this meridionally coherent SL mode dominates interannual SL variability at tide gauges along the North American east coast between 40–50 °N. Hence we conclude that North American coastal sea-level may indeed be a useful indicator of MOC variability on interannual timescales, allowing an observationally-based estimate of the likely range of interannual MOC fluctuations to be determined.

1. Introduction

Previous studies have raised the possibility of using SL observations to diagnose the North Atlantic MOC. In response to a diminished MOC, both *Levermann et al.* [2005] and *Vellinga and Wood* [2007] find that SL rises in the North Atlantic reducing the north-south SL gradient associated with the primarily zonal North Atlantic Current (NAC). *Landerer et al.* [2007] also finds that average SL rises in the North Atlantic in response to an MOC slowdown, but as part of a more complex tri-pole pattern which is attributed to a northward shift in the NAC. This conflicts with [*Hakkinen*, 2001] who finds SL decreases along the path of the NAC due to decreased heat advection by a weakened MOC. These results, while showing the potential of SL as an indicator of MOC variability, also point to the difficulty of untangling the many ways a changing MOC may affect regional SL variability.

According to geostrophy, a more direct relationship exists between the MOC, or, more precisely, the zonal integral of the meridional transport (MT) at a given latitude, and the pressure difference between the east and west boundaries. In fact, in an eddy permitting ocean model, *Bingham and Hughes* [2008] (henceforth BH) find that north of the Gulf Stream (at 42°N) the eastern boundary pressure can be neglected such that the interannual MT variability within a given depth interval is closely approximated by:

$$T \approx -\frac{1}{\rho_0 f_0} \int_{z_2}^{z_1} p_w dz, \qquad (1)$$

where p_w is the bottom pressure (BP) anomaly on the western boundary, ρ_0 is the mean density of seawater, and f_0 is the Coriolis parameter. (Although somewhat counterintuitive, a depth-integral of BP is reasonable since the ocean boundaries have finite gradients so BP is defined at every depth.)

Of course, BP is not as readily observed as SL. This leads us to consider in this letter the relationship between BP and SL along the North Atlantic western boundary. We show how in the eddy-permitting ocean model OCCAM SL on the shelf is closely related to the western boundary BP signal and can therefore be used to determine interannual MT variability. Observational evidence is presented showing how interannual fluctuations in coastal SL north of the Gulf Stream tend to be meridionally coherent, consistent with the model results. This leads us to conclude that North American coastal SL may indeed be a useful indicator of MOC variability.

2. MOC and coastal sea level in OCCAM

[*Bingham et al.*, 2007] have shown that in OCCAM interannual MOC variability north of the Gulf Stream is dominated by single overturning cell with an upper layer above 1300m balanced by a lower layer from 1300m to about 3000m. From 1987 this cell gradually weakens before beginning a recovery in 1994 that persists over the remainder of the model run. (For details of OCCAM see [*Bingham et al.*, 2007] and references therein.)

Given (1), the leading EOF (Empirical Orthogonal Function) of interannual BP variability along the western boundary of the North Atlantic in OCCAM, E_p, is consistent with the variability of the MOC just described. (Figure 1a and the blue curve in 1e). Note how E_p changes sign along the 1300m isobath (the inshore contour in each of the maps) from 35N to the northern limit of the analysis at 55N. The BP amplitude below 1300m is less than it is above because the upper layer transport is balanced by flow in a thicker lower layer. (To isolate interannual variability all fields referred to in this paper were filtered by removing the mean seasonal cycle and applying a 13 month box car filter.)

The leading EOF of SL variability, E_h, (Figure 1b and the red curve in 1e) also varies in phase with the MOC and accounts for over 80% of the SL variability on the shelf north of 35°N (Figure 1d). Like E_p, south of 45°N, E_h changes sign along the continental slope, though not as definitely. Unlike E_p, the amplitude of E_h over the deep ocean is similar to that on the shelf. Yet, tellingly, it still contributes negligibly to the deep ocean variance. This points to a suppression of baroclinic variability by the continental slope.

In OCCAM there is a clear linear relationship between the anomalous MT at 50°N in the upper layer (100-1300m) and coastal SL variability (Figure 2), with a positive (negative) SL anomaly of 2cm corresponding to a 1Sv reduction (increase) in transport (the exact slope is -0.59 Sv/cm). This simple linear regression model of anomalous MT in the upper layer as a function of coastal SL captures 85% of the variance.

As mentioned previously, BH find that in OCCAM the MT variability in the upper layer is balanced by opposing variability in a lower layer. Therefore, it must be the case that the BP anomaly on the western boundary changes sign at 1300m, the depth of the interface between the two layers. This is seen clearly in E_p (Figure 1a). Assuming that p_w changes linearly from some value P_w on the shelf edge at $z_1 = 100$m to zero at $z_2 = 1300$m, from (1) we obtain

$$T \approx -\frac{10^3 P_w}{2\rho_0 f_0} = -\frac{10 g h_w^{cm}}{2 f_0} \approx -\frac{h_w^{cm}}{2}\mathrm{Sv} \tag{2}$$

where we have expressed the pressure P_w in terms of an equivalent water thickness in centimetres h_w^{cm} using $P_w = (\rho_0 g h_w^{cm})/100$ and used the approximate values $g = 10\mathrm{ms}^{-2}$

and $f_0 = 10^{-4}\mathrm{s}^{-1}$. As Figure 1 reveals, on the shelf, BP expressed in equivalent centimetres of water thickness is approximately equal to the change coastal SL. Thus, (2) states that for each sverdrup increase (decrease) in meridional transport, coastal SL falls (rises) by 2cm, in close agreement with the regression model.

3. Observed sea level variability

So far we have established a close link between interannual MOC and coastal SL variability in OCCAM. We now seek to provide evidence for this link in reality. For this purpose we use altimetry SL anomalies produced by Ssalto/Duacs and distributed by Aviso, with support from CNES. We also use monthly mean tide gauge (TG) records from the Permanent Service for Mean Sea Level (PSMSL) to which we applied an inverse barometer (IB) correction. Within the latitude range 40–55°N, excluding those in the St Lawrence river which is not resolved by OCCAM, we found 21 records (inverted triangles in Figure 3a and specified in Figure 4b) covering the 1985 to 2003 period spanned by the OCCAM run. As before, both sets of data were filtered to isolate the interannual variability.

The spatial pattern of the leading EOF, E_a, of the detrended altimetry timeseries (Figures 3a and 3b), is in many respects similar to E_h (Figure 1b). SL on the shelf varies coherently and is in (out of) phase with SL in the deep ocean north (south) of 45°N. Also in agreement with OCCAM, E_a accounts for the majority of the variability on the shelf but little in the interior. However, on the shelf, E_a does not prevail as completely as does E_h. This may reflect the reduced coastal performance of altimetry, or the absence of some small scale processes from OCCAM, or both.

The spatial function of the leading TG EOF, E_t, provides further evidence for a meridionally coherent mode of SL variability along the North American east coast (Figure 3c, red). The amplitude of E_t tends to decrease poleward, as does the fraction of the total variance it accounts for. Yet, E_t still accounts for more then 50% of the variance between Atlantic City at 39°N to Lower Escuminac at 47°N (black and grey inverted triangles in Figure 3a). Repeating the analysis using an equivalent set of data from OCCAM we obtain a leading EOF, E_t^{oc}, whose spatial form resembles that of E_t. However, whereas E_t only accounts for a small part of the variance at the four most northerly stations, E_t^{oc} accounts for the majority of the variance at these stations. Again, this suggests that OCCAM misses some smaller scale influences on SL at these locations.

The greatest difference between OCCAM and the observations of coastal SL lie in their temporal evolution. E_t and E_t^{oc} show a similar decline in coastal SL from a high in 1986/87 to a low in 1989/90 (see Figure 3d). Then, according to E_t, coastal SL rises between 1990 and 1994 before falling again by several centimetres. Coastal SL in OCCAM also shows something of a rise and fall over this period but it is much less pronounced. After 1994, the evolution of coastal sea level in OCCAM differs markedly from reality. Most notably, the abrupt rise in sea level during 1995/96 followed by a similarly steep fall during 1998 is captured by both E_t and E_a, but does not occur in OCCAM. We return to a possible reason for this discrepancy in Section 4.

From Figure 3c we see that the coherent SL mode is most clearly expressed at 10 TGs from New York to Yarmouth (black inverted triangles in Figure 3a). Given the consistency of these records (see Figure 4a), an estimate of past variability of the coherent mode of coastal SL is given by their composite (Figure 4b). We see that the 1995/96 SL fluctuation is fairly typical of the variability of SL along the North American coast, which has a range of 10cm peak to peak, and a standard deviation of 2.5cm. Note the generally poor correspondence between changes in coastal SL and anomalous sea surface temperature [*Rayner et al.*, 2003] on the shelf averaged over the latitude range spanned by the TGs (Figure 4, blue curve). This supports our view that interannual coastal SL variability is generally not steric.

4. Discussion and conclusions

In OCCAM, interannual MOC variability is well determined by BP on the western boundary. And since the western boundary BP is closely related to SL on the shelf, MOC variations can be inferred from SL alone using a linear relationship of 2cm/Sv. MOC related SL variations have a particular spatial pattern, constrained by topography, and meridionally coherent. The similarity between the leading SL EOFs from the model and from altimetry suggest similar underlying dynamics. If so, the abrupt rise of coastal SL during 1994-96 reflects an sudden but temporary slowdown of the MOC. In support of this, *Hakkinen* [2001] describe an abrupt slowdown of the MOC during this period in their model. Yet, OCCAM fails to reproduce this abrupt change. This may be because the model has not reached full equilibrium due to a short spin-up period of only four years, resulting from the computational demands of running a high resolution model.

Without the full spatial information provided by altimetry, we can be less certain of MOC inferences based on the TG data. However, for the altimetry period, the TG records are dominated by the meridionally coherent mode of SL seen in the altimetry data. In addition, the coherent nature of the interannual SL fluctuations over many decades is clear. If we assume the underlying spatial pattern given by altimetry then the interannual fluctuations seen in the composite TG record primarily reflect MOC variability, then using the 2cm/Sv relationship given by OCCAM we can estimate of the likely range of interannual MOC variability to have a standard deviation of 1.25Sv, with changes of up to 5Sv occurring over a few years.

However, caution is required in applying our simple relationship between MOC strength and coastal SL at longer timescales since it is not clear if the assumption that BP variability on the eastern boundary is negligible will remain sound. On the one hand, results from *Greatbatch and Peterson* [1996] (Figs. 3 and 4) and *Landerer et al.* [2007] (Figs. 3 and 6) suggests that western boundary pressure remains dominant. On the other hand, it is possible that significant pressure changes across the basin may be caused by eustatic changes in SL due to mass fluxes or by circulation changes. This is illustrated by *Levermann et al.* [2005] where SL (and by inference BP) is seen to increase on both east and west coasts due to MOC slowdown. Because the SL change is uniform across the basin it is not directly associated with changes in meridional transport, but under our assumption of zero change on the eastern boundary it would be interpreted as such. (This explains why *Levermann et al.* [2005] find a 5cm/Sv relationship between MOC strength coastal SL, much larger than our 2cm/Sv rate. Differencing their east and west coast SL values gives a dependency closers to ours.) Ocean warming may also lead to global SL changes without a corresponding BP change. Therefore, further work is need to establish to what extent our relationship holds at longer timescales.

Having said this, unless balanced by a factor causing a drop in coastal SL, we would expect an 8Sv MOC reduction between 1950 and 2004, as claimed by *Bryden et al.* [2005], to have some signature in SL. Under our interpretation it would imply a 16cm rise in coastal SL, and even more according to *Levermann et al.* [2005]. Yet, our composite TG record of SL has a small downward trend, amounting to a 1cm drop over the same period. Interestingly, the implied slight increase in overturning of 0.5Sv is in line with a number of other recent studies [e.g *Wu et al.*, 2004].

Acknowledgments. This study was supported by the UK NERC thematic RAPID programme, NER/T/S/2002/00439 and NER/T/S/2002/00485, and represents a contribution to the Proudman Oceanographic Laboratory's "Sea-level, bottom pressure, and geodetic oceanography" Programme.

References

Bingham, R. J., and C. W. Hughes (2008), Determining north atlantic meridional transport variability from pressure on the western boundary: A model investigation, *J. Geophys. Res.*, doi:10.1029/2007JC004679, in press.

Bingham, R. J., C. W. Hughes, V. Roussenov, and R. G. Williams (2007), Meridional coherence of the North Atlantic meridional overturning circulation, *Geophys. Res. Lett.*, *34*, L23606, doi:10.1029/2007GL031731.

Bryden, H., H. Longworth, and S. Cunningham (2005), Slowing of the Atlantic Overturning circulation at 25N, *Nature*, *438*, 655–657.

Greatbatch, R., and K. A. Peterson (1996), Interdecadal variability and oceanic thermohaline adjustment, *J. Geophys. Res.*, *101*(C9), 20,467–20,482.

Hakkinen, S. (2001), Variability in sea surface height: A qualitative measure for the meridional overturning in the North Atlantic, *J. Geophys. Res.*, *106*(C7), 13,837–13,848.

Landerer, F., J. Jungclaus, and J. Marotzke (2007), Regional dynamic and steric sea level change in response to the IPCC-A1B scenario, *J. Phys. Oceanogr.*, *37*, 296–312.

Levermann, A., A. Griesel, M. Hofmann, M. Montoya, and S. Rahmstorf (2005), Dynamic sea level changes following changes in the thermohaline circulation, *Clim. Dyn.*, *24*(4), doi:10.1007/s00382-004-0505-y.

Rayner, N. A., D. Parker, E. Horton, C. Folland, L. Alexander, D. Rowell, E. Kent, and A. Kaplan (2003), Global analyses of sea surface temperature, sea ice, and night marine air temperature since the late nineteenth century, *J. Geophys. Res.*, *108*(D14), 4407, doi:10.1029/2002JD002670.

Vellinga, M., and R. Wood (2007), Impacts of thermohaline circulation shutdown in the twenty-first century, *Climate Change*, doi:10.1007/s10584-006-9146-y.

Wu, P., R. Wood, and P. Stott (2004), Does the recent freshening trend in the north atlantic indicate a weakening thermohaline circulation?, *Geophys. Res. Lett.*, *31*, L02301, doi:10.1029/2003GL018584.

Figure 1. The leading EOFs of model interannual bottom pressure (BP) variability (a) and (e, blue) and sea level (SL) variability (b) and (e, red) on the western boundary of the North Atlantic. The spatial functions are scaled by the standard deviation of the temporal function and the temporal function has been normalised by its standard deviation. (c) The percent of interannual BP variance accounted for the leading EOF. (d) Repeating (c) for interannual sea-surface height. Bathymetry is contoured at 1300m and 3000m.

Figure 2. (a) A scatter plot of interannual coastal SL variability against the upper layer transport variability at 50N. (b) The upper layer meridional transport interannual variability at 50N (red), and reconstructed from a linear regression model relating sea level (SL) variability at the coast with the upper layer transport (blue).

Figure 3. (a) The spatial function of the leading interannual sea level (SL) EOF from altimetry, after detrending and low pass filtering. (b) The percent of interannual SL variance accounted for the leading EOF. (c) The spatial function of the leading EOF of tide gauges along the east coast of North America (solid red) and the percent of total variance accounted for at each tide gauge by the leading mode (broken red). A repeat of this analysis using OCCAM SL (blue). (d) The temporal functions of the tide gauge EOF (red), the leading OCCAM tide gauge equivalent EOF (blue), and the leading altimetry EOF (green).

Figure 4. (a) Low-pass filtered timeseries at the 10 tide gauges which are most sensitive to the meridionally coherent sea level mode. (b) A composite timeseries of the selected tide gauges (black) and the trend in this composite over the period 1950–2005 (red). The mean sea surface temperature on the shelf over the latitude range spanned by the selected tide gauges (blue).

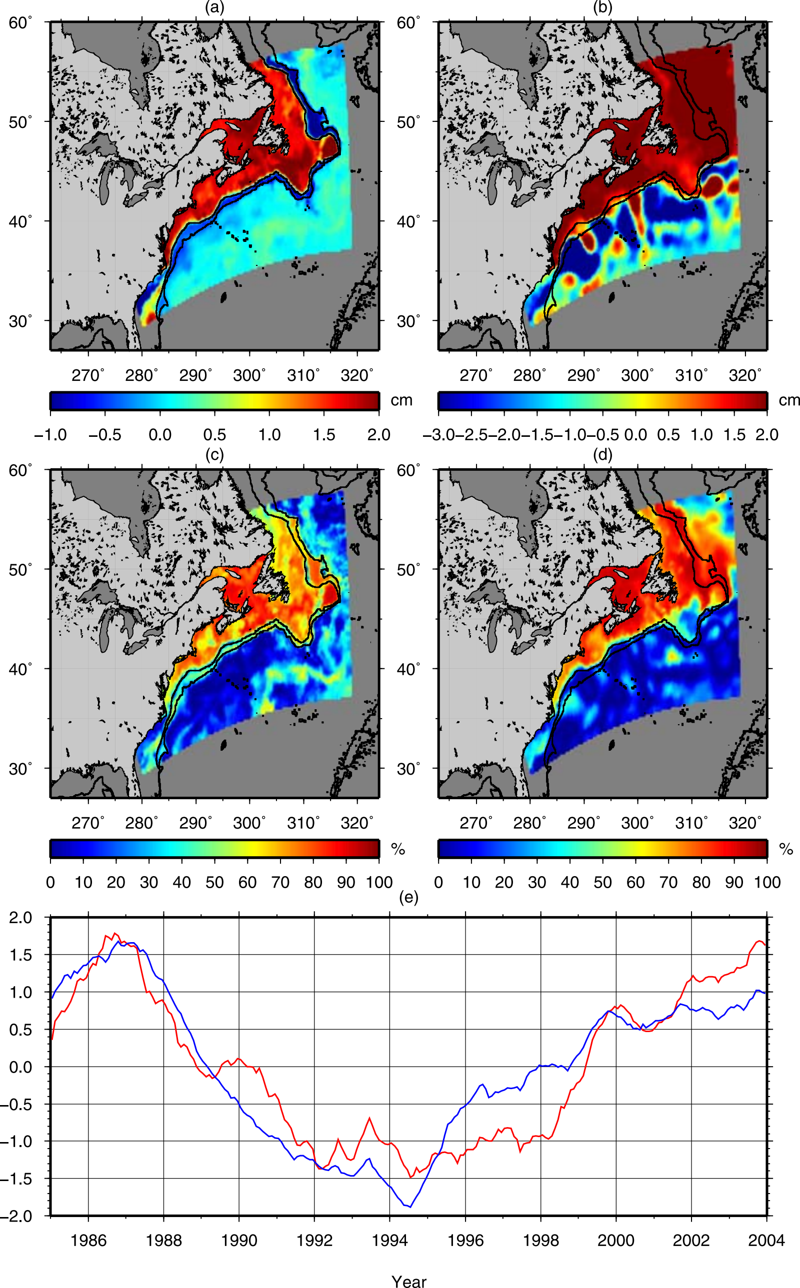

(a)
(b)
(c)
(d)
(e)
60°
50°
40°
30°
270°
280°
290°
300°
310°
320°
cm
−1.0
−0.5
0.0
0.5
1.0
1.5
2.0
−3.0−2.5−2.0−1.5−1.0−0.5 0.0 0.5 1.0 1.5 2.0
%
0 10 20 30 40 50 60 70 80 90 100
2.0
1.5
1.0
0.5
0.0
−0.5
−1.0
−1.5
−2.0
1986
1988
1990
1992
1994
1996
1998
2000
2002
2004
Year

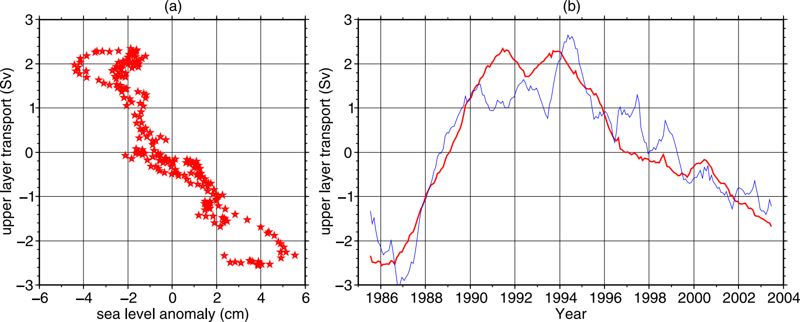
(a)
upper layer transport (Sv)
sea level anomaly (cm)
3
2
1
0
−1
−2
−3
−6
−4
−2
0
2
4
6
(b)
upper layer transport (Sv)
Year
1986
1988
1990
1992
1994
1996
1998
2000
2002
2004

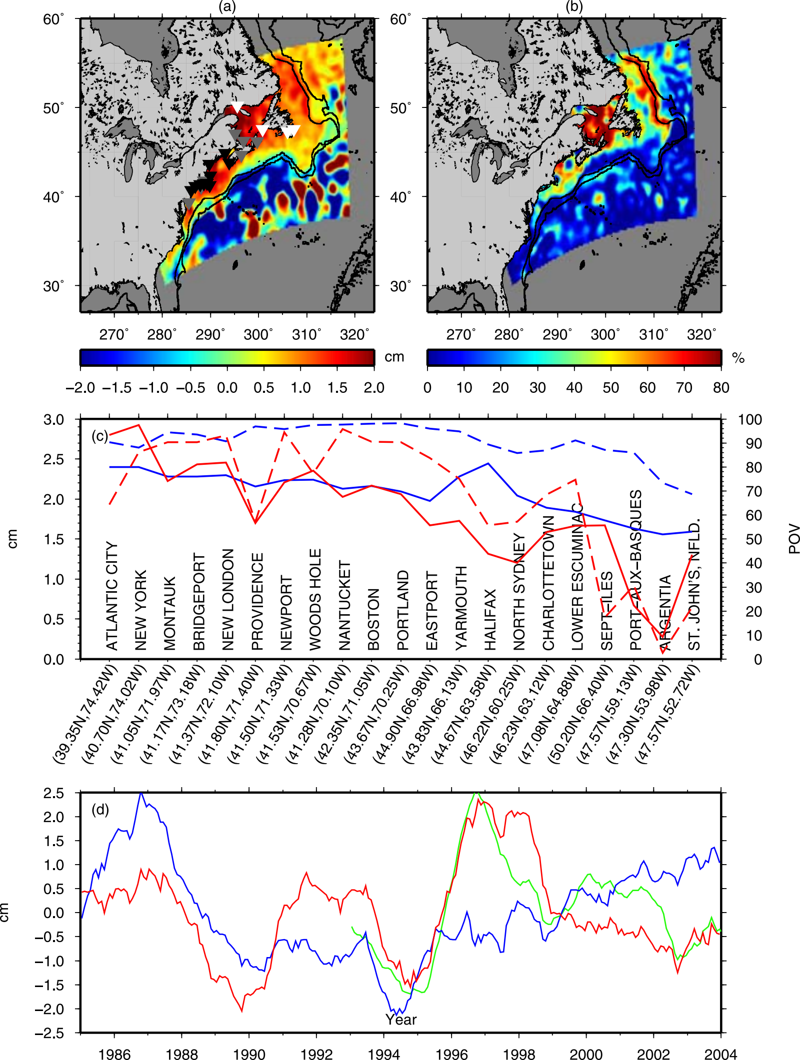

(a)
(b)
60˚
50˚
40˚
30˚
270˚
280˚
290˚
300˚
310˚
320˚
cm
−2.0 −1.5 −1.0 −0.5 0.0 0.5 1.0 1.5 2.0
%
0 10 20 30 40 50 60 70 80
(c)
cm
POV
ATLANTIC CITY
NEW YORK
MONTAUK
BRIDGEPORT
NEW LONDON
PROVIDENCE
NEWPORT
WOODS HOLE
NANTUCKET
BOSTON
PORTLAND
EASTPORT
YARMOUTH
HALIFAX
NORTH SYDNEY
CHARLOTTETOWN
LOWER ESCUMINAC
SEPT–ILES
PORT–AUX–BASQUES
ARGENTIA
ST. JOHN'S, NFLD.
(39.35N,74.42W)
(40.70N,74.02W)
(41.05N,71.97W)
(41.17N,73.18W)
(41.37N,72.10W)
(41.80N,71.40W)
(41.50N,71.33W)
(41.53N,70.67W)
(41.28N,70.10W)
(42.35N,71.05W)
(43.67N,70.25W)
(44.90N,66.98W)
(43.83N,66.13W)
(44.67N,63.58W)
(46.22N,60.25W)
(46.23N,63.12W)
(47.08N,64.88W)
(50.20N,66.40W)
(47.57N,59.13W)
(47.30N,53.98W)
(47.57N,52.72W)
(d)
cm
Year
1986 1988 1990 1992 1994 1996 1998 2000 2002 2004

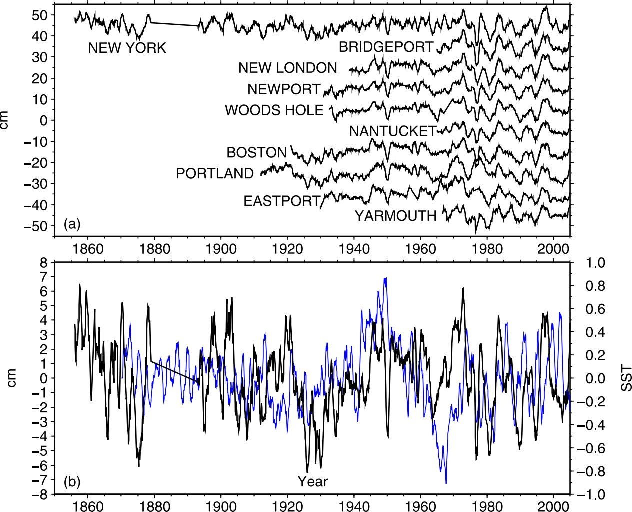

NEW YORK
BRIDGEPORT
NEW LONDON
NEWPORT
WOODS HOLE
NANTUCKET
BOSTON
PORTLAND
EASTPORT
YARMOUTH
(a)
cm
(b)
cm
SST
Year